RESEARCH ARTICLE

Fabrication, Characterization and Degradation of Electrospun Poly(ε-Caprolactone) Infused with Selenium Nanoparticles

Nurul Asyikin Kamaruzaman[a,b], Abdull Rahim Mohd Yusoff[b,*], Nik Ahmad Nizam Nik Malek[c], Marina Talib[d]

[a] National Nanotechnology Centre, Ministry of Science, Technology and Innovation, 62662 Putrajaya, Malaysia; [b] Department of Chemistry, Faculty of Science, Universiti Teknologi Malaysia, 81310 UTM Johor Bahru, Johor, Malaysia; [c] Department of Biosciences, Faculty of Science, Universiti Teknologi Malaysia, 81310 UTM Johor Bahru, Johor, Malaysia; [d] Malaysian Nuclear Agency, Bangi 43000 Kajang, Selangor, Malaysia

Abstract Polycaprolactone (PCL) is widely used in the fabrication of nanofibers through the electrospinning technique. PCL is a biodegradable material that is economical, simple and can be scaled up for industrial production. In this study, PCL was infused with selenium nanoparticles (SeNPs) via electrospinning to fabricate PCL-SeNPs nanofiber. Field emission scanning electron microscopy (FESEM) images of the samples revealed 'aligned fibers' were successfully fabricated with a diameter of less than 350 nm and an average diameter of 185 nm. The presence of Se in the nanofiber was confirmed by energy dispersive X-ray analysis (EDX) and Raman spectra. Based on the X-ray diffraction (XRD) pattern, the structure of PCL did not change and remained in the PCL-SeNPs nanofibers. As indicated by infrared (IR) spectra, the functional groups of PCL remained the same after SeNPs infusion. These results demonstrated that PCL nanofibers' physical and chemical properties were not affected by the infusion of SeNPs. In addition, the hydrophobicity of the PCL decreased slightly in the presence of SeNPs. The first month after degradation, disorganized and fibrous fibers of PCL-SeNPs nanofiber were observed, followed by the formation of large fiber clumps as degradation time increased. An agglomerated SeNPs made PCL-SeNPs nanofiber pores looser and easier to be hydrolyzed after four months of degradation. The sticky surface of PCL-SeNPs nanofiber shows acceleration in the hydrolysis process after 24th weeks of degradation. The presence of SeNPs enhanced the degradation behavior and reduced the degradation time to break into pieces, starting after six months of degradation. The 'aligned' PCL-SeNPs nanofiber, which can mimic the natural tissue extracellular matrix (ECM) morphology, can potentially be used in biomedical applications such as tissue engineering, wound dressing, biomedicine, sensor and filtration application.

Keywords: Fabrication nanofibers, Poly(ε-Caprolactone), Selenium Nanoparticles, Degradation

Introduction

There are many applications of nanofibers from medical to consumer products involving drug delivery

system [1-3], wound dressing [4-8], tissue engineering [9-11], enzyme immobilization [12-15], antibacterial agents [16-21], protective material [22-26], sensors [27-32] and filtration [33-34], which have attracted worldwide researchers.

The fabrication of nanofibers using electrospinning attracted the attention of the researchers due to its economical, easy handling, versatility and ability of electrospinning to continuously produce fibers on nanometers scale [7-8]. Poly(ε-caprolactone) (PCL) is a low-cost biodegradable polymer that has been proven to be a promising material in medical applications [9-10]. Electrospun PCL nanofibers have also contributed special characteristics in many biology applications, such as slower degradation time, nonimmunogenic, extensible, and easily obtainable resources. However, there are limited studies on the fabrication of PCL nanofibers with fillers or additives [11-12].

PCL electrospun can be incorporated with nanoparticles, such as carbon nanotubes, silver, gold, zinc, magnesium, iron, cerium, and chitosan. These nanoparticles have been studied in various biomedical fields, especially for drug delivery, wound dressings and scaffolds [13-21]. Meng *et al.* [13] mentioned that when MWCNTs were infused with PCL to produce electrospun PCL/MWCNTs nanofiber, it was potentially used in a scaffold application due to good degradation, biocompatibility and hemocompatibility. The antibacterial silver nanoparticles can be applied as a wound dressing when incorporated with PCL electrospun [14-15]. Suryavanshi *et al.* mentioned that MgO–PCL electrospun could potentially be used as a scaffold material for bone-soft tissue engineering applications [17]. There was a report that the iron oxide nanoparticles loaded into PCL nanofibers may have a potential application in tissue engineering, specifically as localized drug delivery vehicles [18-19]. Chitosan nanoparticles in PCL electrospun are not only suitable to be used as a material for wound dressing but also for drug delivery [21]. In addition, the *in vitro* degradation of PCL nanofiber incorporated nanoparticles has been studied. It was proven that the existence of nanoparticles improved the time and rate of PCL electrospun degradation [16]. However, some of the nanoparticles, such as silver nanoparticles, were toxic to aquatic life [22-23].

As mentioned in the previous studies, SeNPs possess antimicrobial properties that give advantages in biomedical and healthcare applications. Therefore, SeNPs was chosen to be incorporated in PCL nanofiber due to its biocompatibility, selective toxicity and is well dispersed in the solution [24-25]. Chung *et al*. [26] mentioned that the doping of electrospun silk with selenium nanoparticles improved wound healing and reduced infection without relying on antibiotic treatment]. The mixing of Mg–Se–CHAP and PCL solution using electrospun produced Mg–Se–CHAP/PCL microfibers for potential clinical applications [27]. Kamaruzaman *et al.* [28] mentioned that different concentrations of SeNPs infused in PCL nanofiber through electrospinning could potentially be used for various applications, such as wound dressing and water filtration [28].

This study aims to fabricate PCL-SeNPs nanofiber through the electrospinning technique. The characterizations of the prepared materials were done to observe the effect of structure, wettability, physical and chemical properties of the PCL nanofiber after infusion with SeNPs. The degradation of PCL-SeNPs nanofiber was soaked in the Simulated Body Fluid (SBF) solution for 12 months. The morphology of degraded PCL-SeNPs nanofiber was analyzed to observe the effect of SeNPs in PCL-SeNPs nanofiber during the degradation study.

Materials and methods

Fabrication of PCL-SeNPs nanofiber
The 4.0wt% PCL solution was prepared by dissolving PCL (Sigma-Aldrich) in the mixture of tetrahydrofuran (QRec) and dimethylformamide (QRec) at a ratio of 3:1 under magnetic stirring at 28°C. Then, 0.4wt% of synthesized SeNPs from Kamaruzaman study [28] were mixed in the PCL solution before the solution was sonicated for one hour to obtain a homogenous solution. After that, the electrospinning (Fanavaran) was carried out at 28°C by loading the solution in a syringe and was injected through a stainless-steel blunt-ended needle. The flow rate of the PCL-SeNPs solution was controlled at

2.0 ml/h by a syringe pump. The collector was electrically grounded with a fixed distance between the metal collector and the needle tip at 15 cm under a voltage of 20 kV. Then, SeNPs were incorporated into PCL nanofiber through jet spraying before fibers were formed. The PCL-SeNPs nanofiber was collected at the metal collector and was stored in a desiccator before being characterized. Figure 1 shows the schematic diagram of the electrospinning setup.
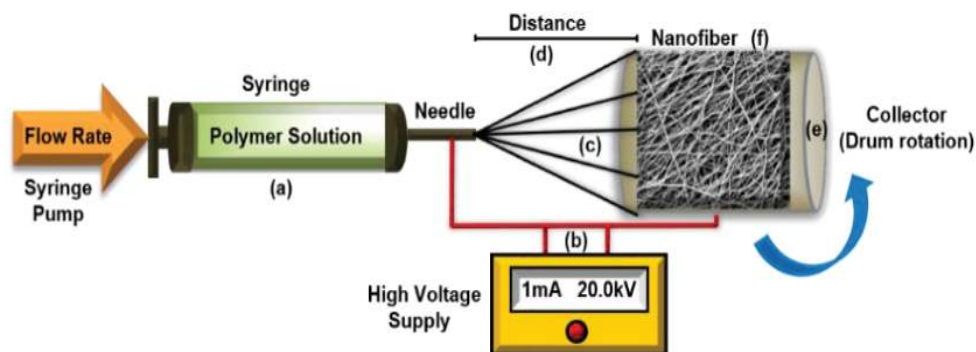

Figure 1: A schematic diagram of the electrospinning set-up. (a) Syringe with polymer solution, (b) high voltage current supply, (c) spinneret, (d) distance between the needle tip and collector, (e) collector and (f) nanofibers.

Characterization Techniques

The structural characterization of the samples was performed using XRD to determine the crystallinity of the samples. The solid product was packed down and leveled off with a glass slide to get a flat and smooth surface. The powder XRD patterns of the sample were measured at room temperature in the range of 5-90° with a D8 ADVANCE X-ray diffractometer (Bruker AXS GmbH). The parameter was set up with Cu Kα radiation (λ = 1.5418Å) at 8.04 kV and the wavelength of *l* = 1.5418 Å with a step size of 0.05°. The applied voltage was 35 kV, and the current was 25 mA.

The samples were characterized using Fourier transform infrared (FTIR) spectroscopy with attenuated total reflectance mode (ATR) in order to confirm the presence of functional groups in the samples. Firstly, the samples were placed on the sample holder, and the FTIR spectra were analyzed at a resolution of 0.4 cm^{-1}. The spectrum was recorded from 4000 to 500 cm^{-1} on an FTIR spectrophotometer (Bruker Tensor II).

The surface morphology of the samples was observed using a field emission scanning electron microscope (FESEM), which was performed on the samples by a scanning electron microanalyzer Zeiss supra 35vp. Firstly, the sample was spread over an aluminum stub using a double-edged tape followed by coating the surface with gold particles. FESEM measurement was carried out the bombardment of 30 KeV energy electrons on the target sample particles. Electrons that are emitted from the specimen with an energy of less than 50 eV are defined as secondary electrons and are used for specimen investigation. This instrument also included detecting scattered X-rays for characteristic radiation of a specific element in an energy dispersive system to identify the elements. The contents of the required elements were determined using the energy dispersive X-Ray (EDX) analysis that was incorporated with the FESEM.

The sample was placed as a thin film on small pieces of aluminum foil and dried in air at 28°C. Raman spectra were acquired with the Renishaw Raman spectrometer (inVia) using 633 nm excitation (30 mW; spectral range 100-3200 cm^{-1}). The acquisition interval was 10 s, and all spectra were averaged over ten independent runs.

Contact angle measurements were performed using the static water contact angle measurements with the sessile drop method using a contact angle measurement system (Biolin Scientific). The sample was placed on a sample holder stage, and one drop of deionized water (1 µL) was placed onto the sample surface. Then, the images of the water droplets were recorded using a video camera system, and the

surface contact angles were calculated based on these images.

Simulated Body Fluid (SBF) was prepared by adding 8.035 g of sodium chloride (NaCl), 0.355 g of sodium bicarbonate (NaHCO$_3$), 0.225 g of potassium chloride (KCl), 0.231 g of potassium phosphate dibasic trihydrate (K$_2$HPO$_4$.3H$_2$O), 0.311 g magnesium chloride hexahydrate (MgCl$_2$.6H$_2$O), 39 mL of 1 M hydrochloric acid (HCl), 0.292 g calcium chloride (CaCl$_2$), 0.072 g sodium sulfate (Na$_2$SO$_4$) and 6.118 g of tris(hydroxymethyl) aminomethane (C$_4$H$_{11}$NO$_3$) into 1 L of distilled water [29]. Each reagent was added one by one after the existing reagent was completely dissolved. About 2 cm × 2 cm area of each nanofiber was placed into a 40 ml of SBF solution. The test tube was then placed in the incubator shaker (New Brunswick Classic C24) for 52 weeks (37°C, 150 rpm). The SBF solution was changed every week and prepared freshly. The morphology of each nanofiber at the required time was analyzed using FESEM. Se, C and O elements were determined using mapping analysis.

Results and discussion

Characterization of the samples
PCL-SeNPs nanofibers were fabricated via the electrospinning technique. XRD pattern of PCL-SeNPs nanofibers shows the diffraction peaks that are corresponding to PCL and SeNPs, which is shown in Figure 2 (a).
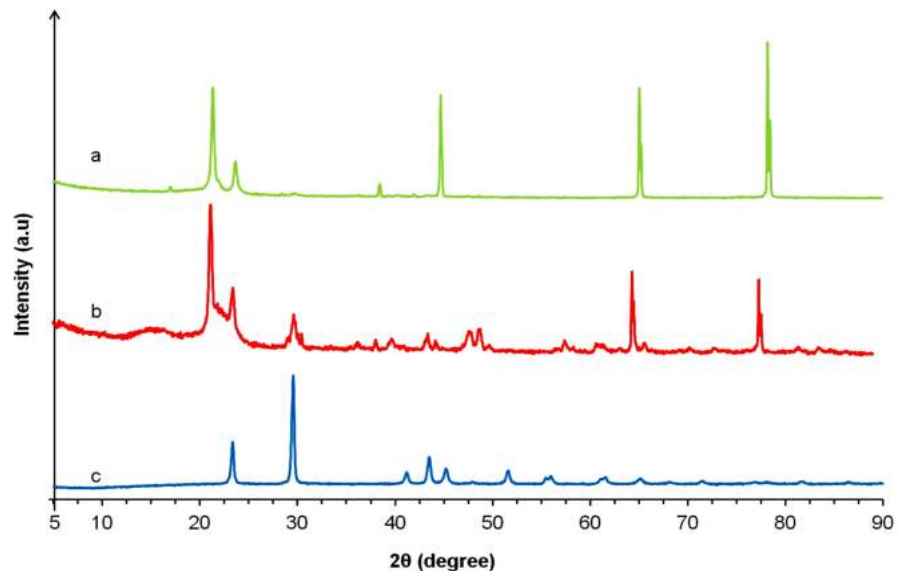

Figure 2: XRD diffractogram of (a) PCL nanofiber, (b) PCL-SeNPs nanofiber and (c) SeNPs.

Figure 2 (b) shows the orthorhombic crystal of PCL, giving strong reflections at 2θ = 21.32°and 23.67° corresponding to the (110) and (200) planes [30-31]. The sample has high crystallinity even though the PCL is a semicrystalline polymer based on the sharp and distinct peaks. However, SeNPs peaks were confirmed by the diffraction peaks at 2θ = 23.67°, 29.94°, 40.20°, 43.86°, 44.69°, 50.13°, 58.09°, 61.29°, 65.05° and 78.15° corresponds to (100), (101), (110), (102), (111), (201), (112), (202), (210) and (113) planes of selenium as shown in Figure 2 (c). All XRD peaks of SeNPs in the PCL-SeNPs nanofibers refer to the trigonal structure of selenium, but some peaks slightly shifted compared to the SeNPs themselves. Hence, it was confirmed that PCL peaks remained in the PCL-SeNPs nanofiber with the presence of SeNPs peaks.

Figure 3 shows the infrared spectra of PCL-SeNPs nanofibers. From the FTIR spectrum, strong bands of the carbonyl stretching mode appeared around 1725 cm^{-1}. Peaks at 1294 cm^{-1} and 1725 cm^{-1} corresponded to the backbone of C-C and C-O stretching modes in the crystalline PCL and carbonyl

vibration regions in amorphous and crystalline forms [34-35]. A strong peak representing C=O appeared at 1725 cm^{-1} while a peak at 1294 cm^{-1} was assigned to C-C and C-O stretching in the PCL-SeNPs nanofibers. However, in this case, these three peaks overlapped at region 1100-1190 cm^{-1}, referring to the amorphous stretching, C–O–C stretching and OC–O stretching for PCL-SeNPs nanofiber [36]. In addition, no peak was observed for Se because Se is an inorganic compound and cannot be confirmed by FTIR analysis. Therefore, only PCL peaks were present in PCL-SeNPs nanofibers. The absence of solvent peaks during electrospinning shows no residual solvent left after fabrication of PCL-SeNPs nanofiber, which might be harmful to biomedical and drug delivery applications. Therefore, XRD and FTIR results confirmed that the infusion of SeNPs in the PCL nanofiber retained the structure and properties of PCL nanofibers and its physical and chemical properties.
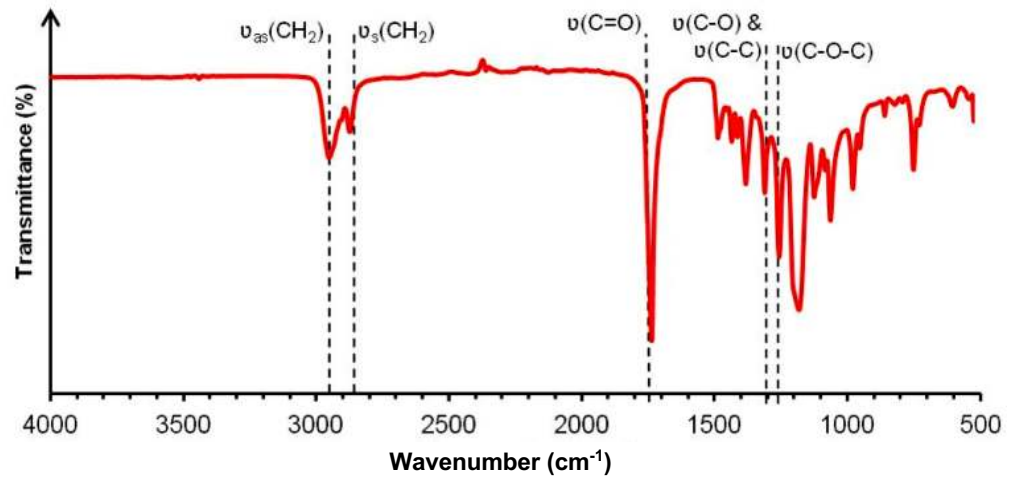

Figure 3. FTIR spectrum of PCL-SeNPs nanofiber.

Figure 4 (a) shows FESEM images of PCL-SeNPs nanofiber with aligned fibers in the presence of spindle-like beads. The PCL-SeNPs nanofiber magnified at 10,000 times, as shown in Figure 4 (b), clearly showed the mixture of straight and corrugated fibers. The straight fibers were produced due to the presence of SeNPs in the PCL-SeNPs nanofiber, increasing the conductivity and electricity of the solution. This results in a continuous path of the injected solution from breaking up and prevents cone shape or droplet formation. The formation of corrugated fibers might be due to splaying jet path or SeNPs in the fiber and coated by PCL solution. The size of fiber diameters was calculated within 70-350 nm with an average length of around 185 nm. The aligned and graded structures of PCL-SeNPs nanofiber depicted a morphology similar to the native extra-cellular matrix (ECM) suitable for tissue engineering applications.
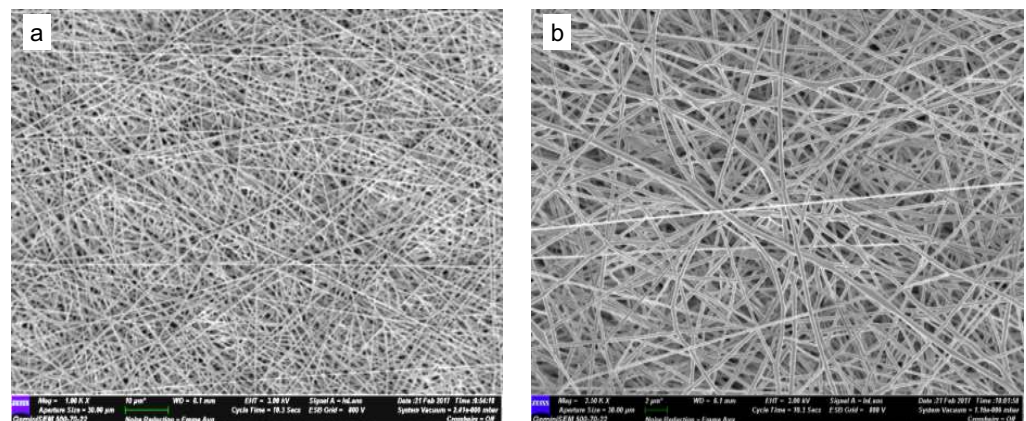

Figure 4: FESEM images of PCL-SeNPs nanofiber at (a) 1,000 and (b) 10,000 magnification.

The presence of SeNPs was confirmed by Se element from EDX result, as shown in Figure 5. The peak located in the spectrum at 1.4 eV was clearly from selenium. However, two peaks between 112 eV and 12.5 eV almost disappeared due to the weak signals detected from the selenium (Se) element compared to carbon (C) and oxygen (O) elements. In addition, there was a small percentage of Se element, which was 3.0% compared to the C element (78.7%) and O element (18.3%). Another reason might be that SeNPs were coated by PCL nanofibers during the electrospinning process and disturbed the signal to detect Se element. As shown in Figure 6, the highest distributions of SeNPs resulted from the spindle-like beads fibers or the junction was produced from two and more fibers in PCL-SeNPs nanofiber. It was confirmed that the existence of SeNPs produced a fiber with spindle-like beads. It might be that during the fabrication of PCL-SeNPs nanofiber, some of the SeNPs still agglomerate due to the nanosize of SeNPs, causing a very strong van der Walls attraction between SeNPs and made it difficult to be separated. About 3% of SeNPs was determined to be in PCL-SeNPs nanofiber, as shown in EDX result. Plus, SeNPs were randomly distributed in the PCL-SeNPs nanofiber due to the excellent dispersion of SeNPs in the PCL solution. However, there are small patches of SeNPs that might be overlapped with many fibers containing SeNPs.
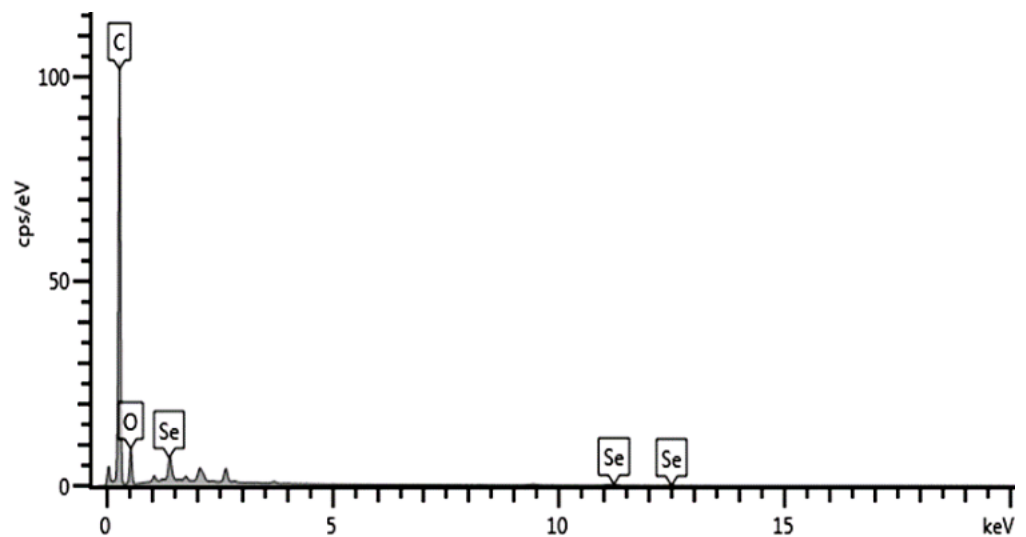

Figure 5. EDX of PCL-SeNPs nanofibers.

The unique characteristics of SeNPs in the Raman spectrum confirmed the presence of SeNPs in PCL-SeNPs nanofiber. The Raman spectrum in Figure 7 showed that the two resonance peaks referred to an intensive single resonance peak around 235 cm^{-1} and a small peak around 144 cm^{-1} [35-37].

The contact angle measurement was done to determine the wettability of the PCL-SeNPs nanofibers surface. From the contact angle images in Figure 8, the surfaces of both PCL and PCL-SeNPs nanofibers are hydrophobic. The degree of hydrophobicity (θ) of PCL nanofiber was ~140°, which is higher compared to PCL nanofiber [38]. It might be due to the effect of a smaller porosity size with a higher fiber density of PCL nanofiber, as seen through the surface morphology image. The smaller fiber sizes produced a higher density of PCL nanofiber, resulting in a smaller pore size. Therefore, the smaller pore sizes than molecule water caused a double effect of hydrophobicity of PCL itself.

The presence of SeNPs in the PCL matrix becomes less hydrophobic, where the hydrophobicity degree of PCL-SeNPs nanofiber was 132.5° compared to PCL nanofibers itself [38-39]. Even though SeNPs did not attach with any functional group, the hydrophobicity of PCL-SeNPs nanofiber significantly decreased when incorporated with SeNPs. This was possibly due to the contact angle that might decrease if functionalized SeNPs were used to incorporate PCL nanofiber.
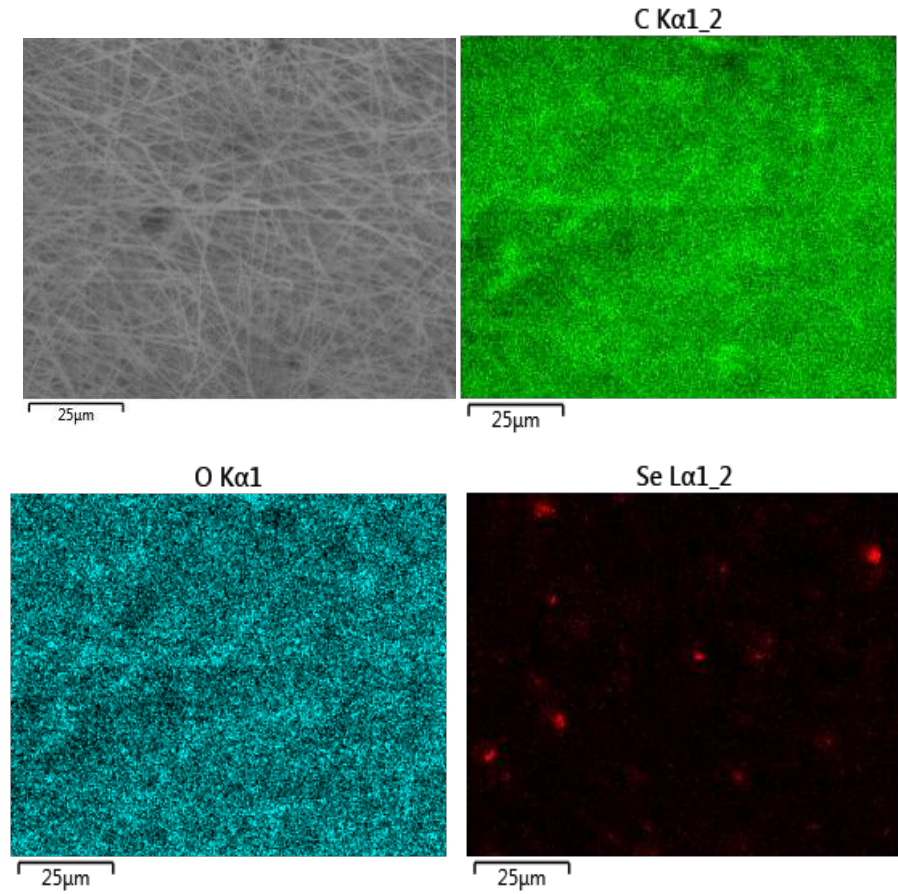
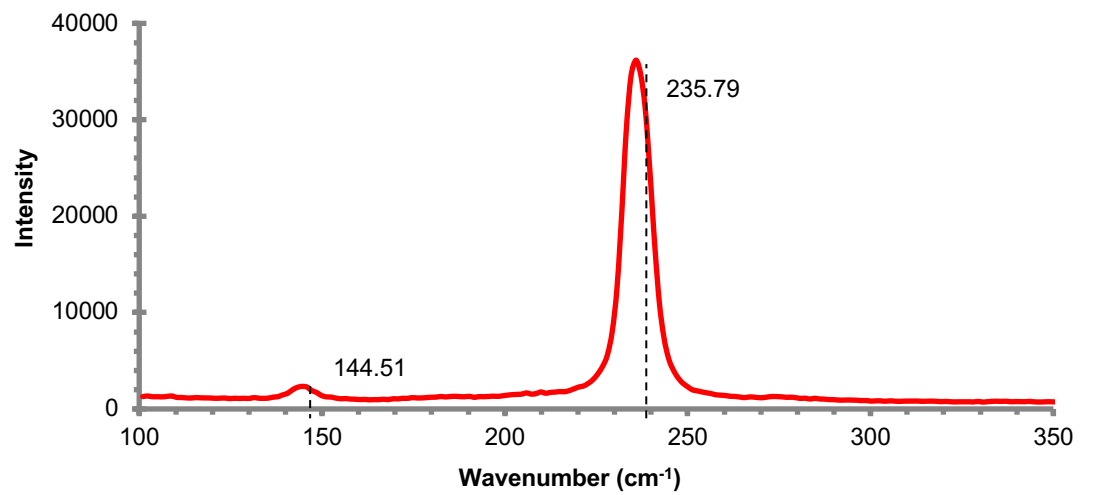**Figure 6.** Elements mapping of PCL-SeNPs nanofibers image.

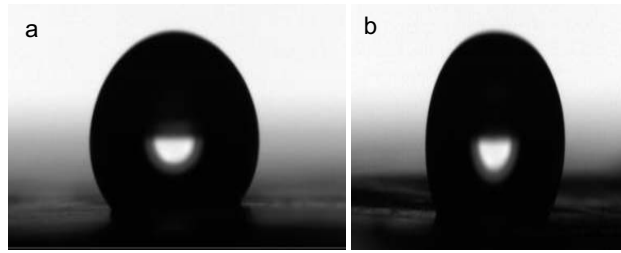**Figure 7.** Raman spectra of PCL-SeNPs nanofiber.

Figure 8. Contact angle of (a) PCL and (b) PCL-SeNPs nanofibers.
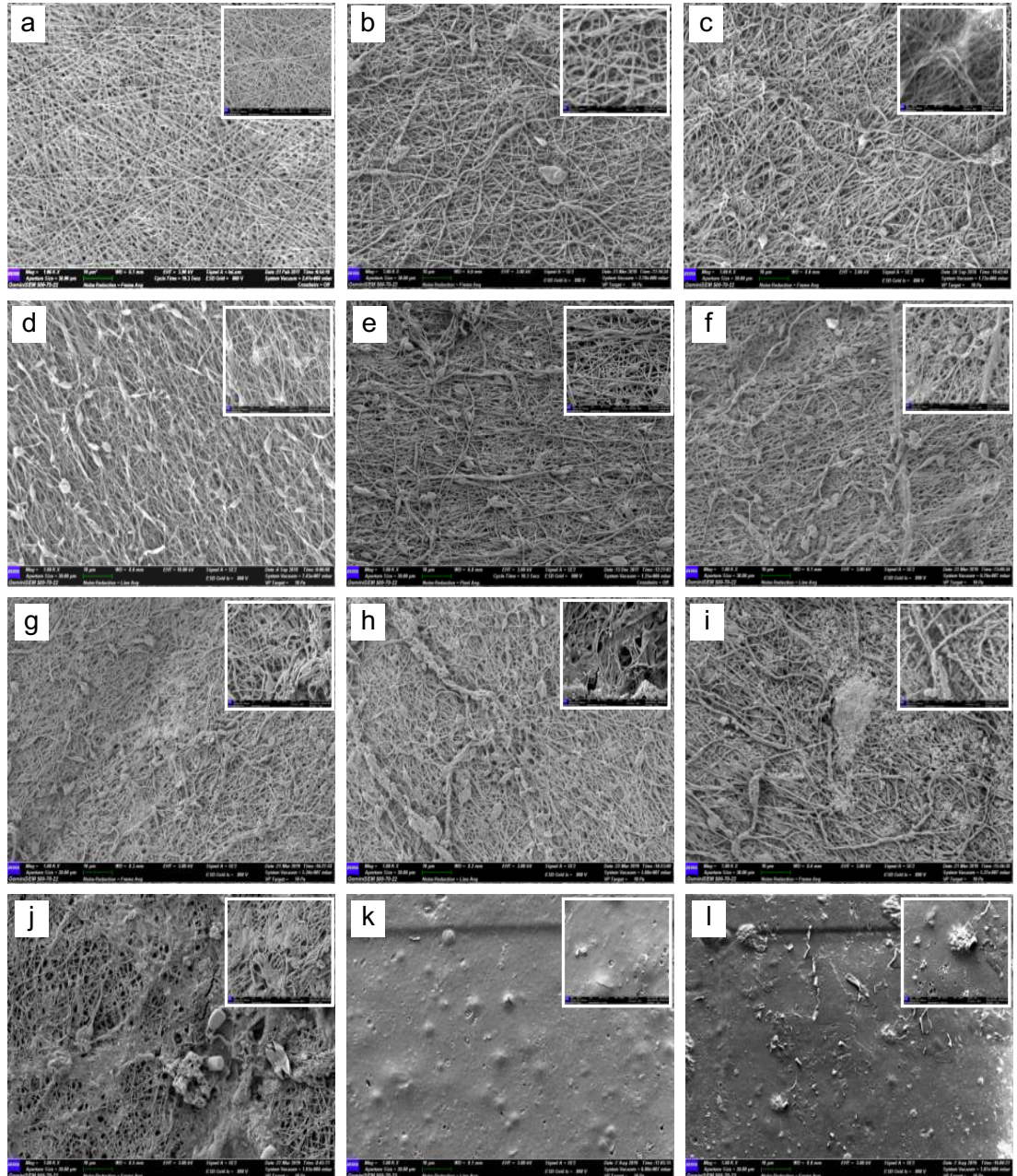

Figure 9. FESEM images of PCL-SeNPs nanofibers (a) before and after (b) 1, (c) 2, (d) 3, (e) 4, (f) 8, (g) 12, (h) 16, (i) 20, (j) 24, (k) 36 and (l) 52 weeks of degradation studies.

Degradation Analysis

Changes in the PCL-SeNPs nanofiber surface morphology before and after degradation in SBF solution within 52 weeks are shown in Figure 9. Some minor changes in the surface morphology of PCL-SeNPs nanofiber occurred. Disorganized and fibrous fibers were observed after a week of degradation. It can be seen that the fibers were accumulated and began to clump with each other, causing a formation of a fibers network surrounding it.

Beads were formed after the second week of degradation, as seen in Figure 9 (c). The number of beads was also increased simultaneously, with large fiber clumps forming as degradation time increased. Then, the fibers were continued to clump, resulting in a fibers network until sixteen weeks of degradation (Figure 9 (h)). The existence of beads was decreased and attached to form an extensive clumped network of the fibers. At the same time, the structure started to break due to the hydrolysis process of the PCL. SeNPs were agglomerated before creating a bunch of groups at twenty weeks of degradation. This is because the nano size of SeNPs will agglomerate due to the very strong van der Wall attraction between SeNPs. In addition, the attachment of SeNPs onto the fibers was confirmed by FESEM images at 5,000 times. Hence, the presence of SeNPs in the PCL-SeNPs nanofiber enhanced the degradation behavior even though small pores made it difficult for the molecules of water to diffuse into it. As can be seen from the sticky surface of PCL-SeNPs nanofiber in Figure 9 (j), the acceleration of the hydrolysis process of PCL occurred after the 24th week of degradation. The surface begins to be bumpy in the appearance of cracks, and physically PCL-SeNPs nanofiber was degraded into small pieces. After 36 weeks of degradation, small holes were produced while rough and scalp surfaces were observed at 52 weeks of PCL-SeNPs nanofiber degradation. At this stage, PCL-SeNPs nanofiber becomes more brittle and easier to break into pieces compared to 36 weeks of degradation.

Conclusions

This study successfully fabricated PCL-SeNPs nanofibers via electrospinning by infusing SeNPs (0.6%wt) into a 4%wt PCL solution. The aligned fibers were fabricated in the presence of a bead, with the diameter of the fibers was less than 350 nm. The structure, physical and chemical properties of PCL nanofibers remained in the presence of SeNPs. However, the hydrophobicity of PCL-SeNPs nanofibers decreased slightly compared to PCL nanofibers. PCL-SeNPs nanofibers began to degrade after 6 months in the SBF solution, which could potentially be applied in tissue engineering, wound dressing, biomedicine, sensor and filtration applications.

Conflicts of interest

The authors declare that there is no conflict of interest regarding the publication of this paper.

References

[1] Z. Ma, W. He, T Yong and S. Ramakrishna, "Grafting of gelatin on electrospun poly(caprolactone) nanofibers to improve endothelial cell spreading and proliferation and to control cell Orientation," Tissue Engineering, vol. 11, no. 7-8, pp. 1149–1158, 2005.

[2] H. S. Kim and H. S.Yoo, "MMPs-responsive release of DNA from electrospun nanofibrous matrix for local gene therapy: in vitro and in vivo evaluation," J. Control Release, vol. 145, no. 3, pp. 264–271, 2010.

[3] A. Cooper, R. Oldinski, H. Ma, J. D. Bryers and M. Zhang, " Chitosan-based nanofibrous membranes for antibacterial filter applications, Carbohydr Polym, vol. 92, no. 1, pp. 254–259, 2013.

[4] N. Bhardwaj and S. C. Kundu, "Electrospinning: a fascinating fiber fabrication technique," Biotech. Adv., vol. 28, no. 3, pp. 325–347, 2010.

[5] M. Baniasadi, J. Huang, Z. Xu, S. Morena, X. Yang, J. Chang, M. A. Quevedo-Lopez, M. Naraghi and M. Minary-Jolandan, "High-performance coils and yarns of polymeric piezoelectric nanofibers," ACS Appl. Mater. Interfaces, vol. 7, no. 9, pp. 5358–5366, 2015.

[6] S. Nasreen, S. Sundarrajan, S. Nizar, R. Balamuragan and S. Ramakrishna, " Advancement in electrospun nanofibrous membranes modification and their application in water treatment," Membranes, vol. 3, no. 4, pp. 266–284, 2013.

[7] D. H. Reneker and H. Fong, "Investigation of the formation of carbon and graphite nanofiber from mesophase pitch nanofiber precursor," Polymeric Nanofiber. American Chemical Society Publishers, Washington, 2006.

[8] J. Fang, H. Wang, H. Niu T. Lin and X. Wang, "Evolution of fiber morphology during Electrospinning," J. Appl. Polym. Sci., Vol.118, no. 5, pp. 2553-2561, 2010.

[9] M. P. Prabhakaran, J. Venugopal, C. K. Chan and S. Ramakrishna, "Surface modified electrospun nanofibrous scaffolds for nerve tissue engineering," Nanotechnol., vol. 19, no. 45, Article ID 455102, 2008.

[10] V. Beachley and X. Wen, "Polymer nanofibrous structures: Fabrication, biofunctionalization, and cell interactions," Prog. Polym. Sci., vol. 35, pp 868-892, 2010.

[11] P. Zhao, H. Jiang, H. Pan, K. Zhu and W. Chen, "Biodegradable fibrous scaffolds composed of gelatin coated poly(epsilon-caprolactone) prepared by coaxial Electrospinning," J. Biomed. Mater. Res. A, vol. 83, no. 2, pp. 372-382, 2007.

[12] M. A. D. Boakye, N. P. Rijal, U. Adhikari and N. Bhattarai, "Fabrication and Characterization of Electrospun PCL-MgO-Keratin-Based Composite Nanofibers for Biomedical Applications," Mater., vol. 8, no. 7, pp. 4080-4090, 2015.

[13] Z. X. Meng, W. Zheng W, L. Li and Y. F. Zheng, "Fabrication and characterization of three-dimensional nanofiber membrance of PCL–MWCNTs by Electrospinning," Mater. Sci. Eng. C, vol. 30, pp. 1014–1021, 2010.

[14] R. H. Dong, Y. X. Jia, C. C. Qin , L. Zhan, X. Yan, L. Cui, Y. Zhou, X. Jiang and Y. Z. Long, "In situ deposition of a personalized nanofibrous dressing via a handy electrospinning device for skin wound care," Nanoscale, vol. 8, 3482-3488, 2016.

[15] R. Thomas, K. R. Soumya, J. Mathew and E. K. Radhakrishnan, "Electrospun Polycaprolactone Membrane Incorporated with Biosynthesized Silver Nanoparticles as Effective Wound Dressing Material," Appl. Biochem. Biotechnol., vol. 176, no. 8, pp. 2213-24, 2015.

[16] R. Augustine, N. Kalarikkal and S. Thomas, "Effect of zinc oxide nanoparticles on the in vitro degradation of electrospun polycaprolactone membranes in simulated body fluid". Int. J. Polym. Mater., vol. 65, no. 1, pp. 28-37, 2015.

[17] A. Suryavanshi, K. Khanna, K. R. Sindhu, J. Bellare and R. Srivastava, "Magnesium oxide nanoparticle-loaded polycaprolactone composite electrospun fiber scaffolds for bone-soft tissue engineering applications: in-vitro and in-vivo evaluation," Biomed Mater., vol. 12, no. 5, Article ID 055011, 2017.

[18] D. Demir, D. Güreş, T. Tecim , R. Genç and N. Bölgen, "Magnetic nanoparticle-loaded electrospun poly(ε-caprolactone) nanofibers for drug delivery applications," Appl. Nanosci., vol. 8, no. 6, pp.1461-1469, 2018.

[19] A. S. Perera, S. Zhang, S. Homer-Vanniasinkam, M. O.Coppens and M. Edirisinghe, "Polymer–Magnetic Composite Fibers for Remote-Controlled Drug Release," ACS Appl. Mater. Interfaces, vol. 10, pp. 15524−15531, 2018.

[20] H. A. Rather, R. Thakore, R. Singh, D. Jhala, S. Singh and R. Vasita, "Antioxidative study of Cerium Oxide nanoparticle functionalised PCL-Gelatin electrospun fibers for wound healing application" Bioactive Mater., vol. 3, pp. 201-211, 2018.

[21] S. M. Jung, G. H. Yoon, H. C. Lee and H. S. Shin, "Chitosan nanoparticle/PCL nanofiber composite for wound dressing and drug delivery, " Biomater. Sci. Polym. Ed.,vol. 26, no. 4, pp. 252-263, 2015.

[22] R. Kalbassi, S. A. Johari, M. Soltani and I. J. Yu, "Chitosan nanoparticle/PCL nanofiber composite for wound dressing and drug delivery. Biomater. Sci. Polym. Ed.," Ecopersia, vol. 1, no. 3,pp. 273-290, 2013.

[23] M. R. Kalbassi, H. Salari-joo and A. Johari, "Toxicity of silver nanoparticles in aquatic ecosystems: salinity as the main cause of reducing toxicity," Iranian Journal of Toxicological, vol. 5, pp. 436-443, 2011.

[24] M. Shakibaie, H. Forootanfar, Y. Golkari T. Mohammadi-Khorsand and M. R. Shakibaie., "Anti-biofilm activity of biogenic selenium nanoparticles and selenium dioxide against clinical isolates of Staphylococcus aureus, Pseudomonas aeruginosa, and Proteus mirabilis," J. Trace Elements Med. Biol., vol. 29, pp 235-241, 2015.

[25] P.A. Tran, N. O. Simpson, E. C. Reynolds, N. Pantarat, D. P. Biswas and A. J. O'Connor, "Low cytotoxic trace element selenium nanoparticles and their differential antimicrobial properties against *S. aureus* and *E. coli*," J. Nanotechnol., vol. 27, no. 4, Article ID 45101, 2016.

[26] S. Chung, B. Ercan, A. K. RoyT. J. Webster, "Addition of Selenium Nanoparticles to Electrospun Silk Scaffold Improves the Mammalian Cell Activity While Reducing Bacterial Growth," Front. in Physiol., Vol.7, pp. 1–6, 2016.

[27] M. K. Ahmed, S. F. Mansour, R. Al-Wafi, S. I. El-dek and V. Uskokovic, "Tuning the mechanical, microstructural, and cell adhesion properties of electrospun epsilon-polycaprolactone microfibers by doping selenium-containing carbonated hydroxyapatite as a reinforcing agent with magnesium ions," *J. Mater. Sci.,* vol. 54, pp. 14524–14544, 2019.

[28] N. A. Kamaruzaman, A. R. M. Yusoff, N. A. Buang and N. G. N. Salleh, "Effects on diameter and morphology of polycaprolactone nanofibers infused with various concentrations of selenium nanoparticles," AIP Conference Proceedings, vol. 1901, no. 1, Article ID 020013, 2017.

[29] M. R. C. Marques, R. Loebenberg and M. Almukainzi. Simulated Biological Fluids with Possible Application in Dissolution Testing. Dissolution Technologies, vol. 18, no 3, pp. 15-28, 2011.

[30] K. H. Lee, H. Y. Kim, S. M. Khil, Y. M. Ra and D. R. Lee, "Characterization of nano-structured poly(ε-caprolactone) nonwoven mats via Electrospinning," Polymer, vol. 44, no. 4, pp. 187-1294, 2013.

[31] C. K. Senthil Kumaran, "Investigations on selenium and copper nanoparticles for biological applications," Chennai, India, 2014.

[32] M. M. Coleman and J. Zarian, "Fourier-transform infrared studies of polymer blends. II. Poly(ε-caprolactone)–poly(vinyl chloride) system," *J. Polym. Sci. Polym. Phys. Ed.* Vol. 17, no. 5, pp. 837–850, 1979.

[33] Y. He and Y. Inoue, "Novel FTIR method for determining the crystallinity of poly(epsilon-caprolactone),"Polym. Int., vol. 49, no. 6, pp. 623–626, 2000.

[34] J. E. Oliveira, L. H. C. Mattoso, W. J. Orts and E. S. Medeiros, "Structural and Morphological Characterization of Micro and Nanofibers Produced by Electrospinning and Solution Blow Spinning: A Comparative Study," Adv. Mater. Sci. Eng., vol. 1, pp 1-13, 2013.

[35] S. Malhotra, N. Jha and K. Desai, "A Superficial Synthesis of Selenium Nanospheres using Wet Chemical Approach," International Journal Nanotechnology Applied, vol. 3, no. 4, pp. 7–14, 2014.

[36] K. Nagata, K. Ishibashi and Y. Miyamoto, "Raman and Infrared Spectro of Rhombohedral Selenium," Jpn. J. Appl. Phys., vol. 20, no. 3, 463-469, 1981.

[37] A. Husen and K. S. Siddiq, "Plants and microbes assisted selenium nanoparticles: characterization and application," J. Nanobiotechnology, vol. 12, no. 28, pp. 463-469, 2014.

[38] W. T. Su and Y. A. Shih, "Nanofiber containing carbon nanotubes enhanced PC12 cell proliferation and neuritogenesis by electrical stimulation" *Biomed. Mater.Eng.* vol. 26, pp. 189 – 195, 2015.

[39] A. Wesełucha-Birczyńska, M. Świętek, E. Sołtysiak, P. Galiński, K. Piekara and M. Błażewicz, "Raman spectroscopy and the material study of nanocomposite membranes from poly(ε-caprolactone) with biocompatibility testing in osteoblast-like cells*,"* Analyst, vol. 140, pp. 2311–232, 2015.